The EMBO Journal (2009) 28, 1170–1179 | © 2009 European Molecular Biology Organization | All Rights Reserved 0261-4189/09
www.embojournal.org

THE EMBO JOURNAL

Synaptic removal of diacylglycerol by DGKζ and PSD-95 regulates dendritic spine maintenance

Karam Kim[1], Jinhee Yang[1], Xiao-Ping Zhong[2,3], Myoung-Hwan Kim[1], Yun Sook Kim[4], Hyun Woo Lee[1], Seungnam Han[1], Jeonghoon Choi[1], Kihoon Han[1], Jinsoo Seo[5], Stephen M Prescott[6], Matthew K Topham[6], Yong Chul Bae[4], Gary Koretzky[7,8], Se-Young Choi[5] and Eunjoon Kim[1,*]

[1]National Creative Research Initiative Center for Synaptogenesis and Department of Biological Sciences, Korea Advanced Institute of Science and Technology (KAIST), Daejeon, Republic of Korea, [2]Department of Pediatrics, Duke University Medical Center, Durham, NC, USA, [3]Department of Immunology, Duke University Medical Center, Durham, NC, USA, [4]BK21 Program, Department of Anatomy and Neurobiology, School of Dentistry, Kyungpook National University, Daegu, Republic of Korea, [5]BK21 Program, Department of Physiology, College of Dentistry and Dental Research Institute, Seoul National University, Seoul, Republic of Korea, [6]Huntsman Cancer Institute and Department of Internal Medicine, University of Utah, Salt Lake City, UT, USA, [7]Department of Pathology and Laboratory Medicine, University of Pennsylvania School of Medicine, Philadelphia, PA, USA and [8]Department of Medicine, University of Pennsylvania School of Medicine, Philadelphia, PA, USA

Diacylglycerol (DAG) is an important lipid signalling molecule that exerts an effect on various effector proteins including protein kinase C. A main mechanism for DAG removal is to convert it to phosphatidic acid (PA) by DAG kinases (DGKs). However, it is not well understood how DGKs are targeted to specific subcellular sites and tightly regulates DAG levels. The neuronal synapse is a prominent site of DAG production. Here, we show that DGKζ is targeted to excitatory synapses through its direct interaction with the postsynaptic PDZ scaffold PSD-95. Overexpression of DGKζ in cultured neurons increases the number of dendritic spines, which receive the majority of excitatory synaptic inputs, in a manner requiring its catalytic activity and PSD-95 binding. Conversely, DGKζ knockdown reduces spine density. Mice deficient in DGKζ expression show reduced spine density and excitatory synaptic transmission. Time-lapse imaging indicates that DGKζ is required for spine maintenance but not formation. We propose that PSD-95 targets DGKζ to synaptic DAG-producing receptors to tightly couple synaptic DAG production to its conversion to PA for the maintenance of spine density.

The EMBO Journal (2009) **28,** 1170–1179. doi:10.1038/emboj.2009.44; Published online 19 February 2009
Subject Categories: signal transduction; neuroscience
Keywords: DGKζ; diacylglycerol kinase; phosphatidic acid; PSD-95; spine

*Corresponding author. Department of Biological Sciences, Korea Advanced Institute of Science and Technology, 373-1 Guseoung-dong, Yuseong-gu, Daejeon 305-701, Republic of Korea. Tel.: +42 350 2633; Fax: +42 350 8127; E-mail: kime@kaist.ac.kr

Received: 15 August 2008; accepted: 27 January 2009; published online: 19 February 2009

Introduction

Activation of various surface receptors including G protein-coupled receptors (GPCRs) and receptor tyrosine kinases leads to the hydrolysis of phosphatidylinositol 4,5-bisphosphate (PIP_2) (Sternweis *et al*, 1992; Rhee, 2001). PIP_2 hydrolysis is mediated by phospholipase C (PLC) enzymes and produces diacylglycerol (DAG) and inositol 1,4,5-triphosphate (IP_3). Although IP_3 induces Ca^{2+} release from intracellular stores, DAG binds and stimulates various C1 domain-containing effector proteins including protein kinase C (PKC).

The generation and removal of DAG at various subcellular sites occur rapidly (within seconds), indicating a tight regulation of signal termination. The main mechanism for the termination of DAG signalling is to phosphorylate DAG and convert it to phosphatidic acid (PA) by diacylglycerol kinases (DGKs), enzymes conserved in most eukaryotic species (Topham, 2006; Sakane *et al*, 2007). However, it is not well understood how DGKs are targeted to subcellular sites and involved in the tight regulation of local DAG levels.

The excitatory neuronal synapse is a prominent site of receptor activation and signal transduction. Production of DAG at synapses occurs through the activation of PLC-coupled GPCRs, including metabotropic glutamate receptors (mGluRs) (Conn and Pin, 1997). Strong synaptic PLC activation is also triggered by non-GPCRs such as NMDA receptors (NMDARs), a key mediator of excitatory synaptic transmission (Reyes-Harde and Stanton, 1998; Choi *et al*, 2005; Horne and Dell'Acqua, 2007).

Excitatory synapses are mainly localized in spines, which are actin-rich tiny protrusions on neuronal dendrites that exhibit structural and functional interplay with excitatory synaptic transmission (Nimchinsky *et al*, 2002; Tsay and Yuste, 2004; Carlisle and Kennedy, 2005; Ethell and Pasquale, 2005; Govek *et al*, 2005; Hayashi and Majewska, 2005; Matus, 2005; Calabrese *et al*, 2006; Tada and Sheng, 2006; Alvarez and Sabatini, 2007; Schubert and Dotti, 2007; Sekino *et al*, 2007; Bourne and Harris, 2008; Cingolani and Goda, 2008). Because dendritic spines are spatially isolated from dendrites through a narrow neck and have a relatively small volume compared with dendrites, the removal of synaptic signalling molecules may be a key mechanism determining the intensity and time course of postsynaptic responses. In this context, although the mechanisms underlying synaptic Ca^{2+} removal are relatively well understood (Sabatini *et al*, 2001), little is known about how synaptic DAG is efficiently removed.

PSD-95 is an abundant scaffolding protein at excitatory synapses implicated in the regulation of synapse formation, maturation, and structural and functional plasticity (Kennedy, 2000; Scannevin and Huganir, 2000; Funke *et al*, 2004; Elias and Nicoll, 2007; Sheng and Hoogenraad, 2007). These PSD-95 functions are thought to be mediated in part by its interaction with various synaptic signalling proteins and

organization of efficient signalling pathways. For instance, PSD-95 simultaneously binds NMDARs and neuronal nitric oxide synthase to promote the functional coupling between activated receptors and downstream effectors (Brenman *et al*, 1996; Sattler *et al*, 1999). However, involvement of PSD-95 in the termination of synaptic signalling, which is as important as signal activation, is not well understood.

Here, we present data supporting that PSD-95 promotes synaptic recruitment of DGKζ, a DGK isoform enriched at excitatory synapses. Spine density in cultured neurons is regulated by overexpression and knockdown of DGKζ in a manner requiring the catalytic activity and PSD-95 binding. Moreover, deficiency of DGKζ expression in mice leads to reductions in spine density and excitatory synaptic transmission. These results suggest that the conversion of synaptic DAG to PA by the concerted action of DGKζ and PSD-95 is important for the maintenance of normal synaptic density and transmission.

Results

PSD-95 interacts with and promotes synaptic localization of DGKζ

To better understand the PSD-95-dependent molecular organization of excitatory synapses, we searched for PSD-95-binding proteins by yeast two-hybrid screen. The screen identified DGKζ, 1 of the 10 mammalian DGKs (type IV) with a unique C-terminal PDZ domain-binding motif (Figure 1A) (Goto and Kondo, 1996). Additional two-hybrid assays confirmed a specific interaction between the DGKζ C terminus and PDZ domains of PSD-95 family proteins (PSD-95, SAP97, PSD-93/chapsyn-110, and SAP102) (Supplementary Figure S1A). DGKζ did not interact with other PDZ domains from Shank1, GRIP2, PICK1, and nNOS, suggesting that DGKζ interacts selectively with PSD-95 family proteins. DGKζ and PSD-95 family proteins formed complexes in heterologous cells and rat brain (Supplementary Figure S1B; Figure 1B and C).

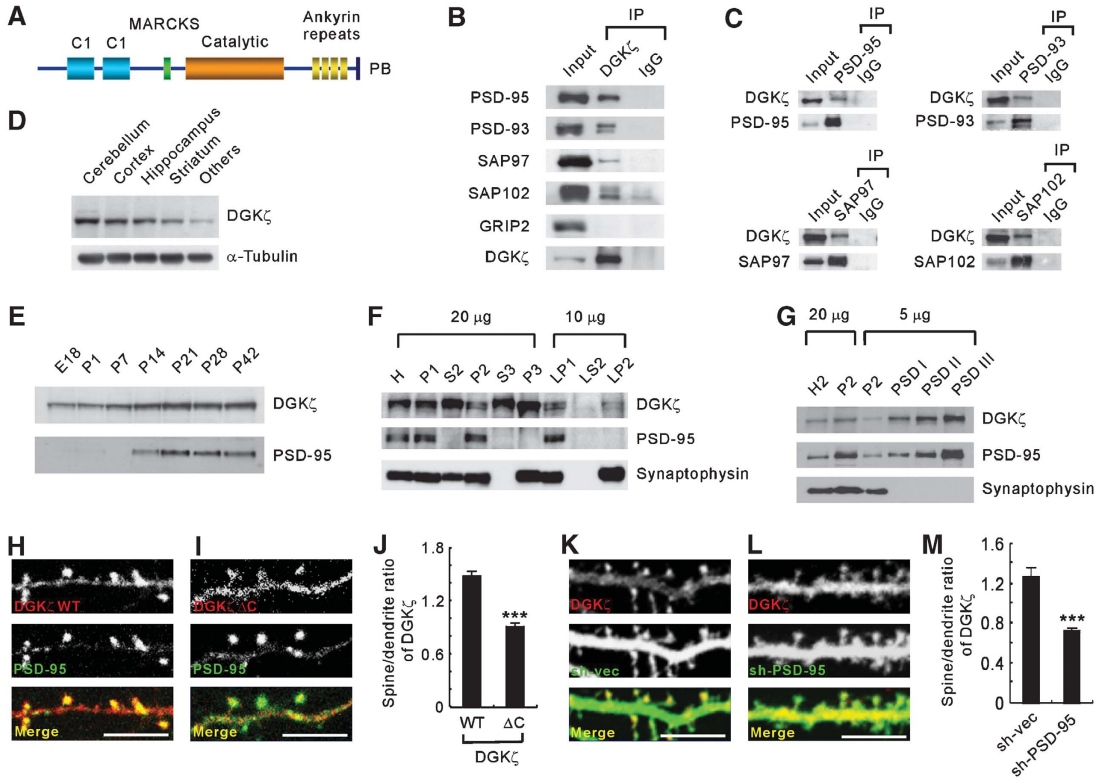

Figure 1 PSD-95 interacts with and promotes synaptic localization of DGKζ. (**A**) Domain structure of DGKζ. C1, protein kinase C conserved region 1; MARCKS, myristoylated alanine-rich C-kinase substrate domain; PB, PDZ domain-binding motif. (**B**, **C**) Association of DGKζ with PSD-95 family proteins *in vivo*. Adult rat brain lysates, solubilized by 1% sodium deoxycholate, were immunoprecipitated with DGKζ antibodies (1519) and immunoblotted with the indicated antibodies. Input, 10%; IP, immunoprecipitation. (**D**) Widespread distribution of DGKζ in various brain regions. α-tubulin was used for normalization. (**E**) DGKζ expression increases during postnatal rat brain development. E, embryonic day; P, postnatal day. PSD-95 was visualized for comparison. (**F**) Distribution patterns of DGKζ in subcellular fractions of adult rat brain. H, homogenates; P2, crude synaptosomes; S2, supernatant after P2 precipitation; S3, cytosol; P3, light membranes; LP1, synaptosomal membranes; LS2, synaptosomal cytosol; LP2, synaptic vesicle-enriched fraction. PSD-95 and synaptophysin were visualized for comparison. (**G**) Enrichment of DGKζ in postsynaptic density (PSD) fractions; extracted with Triton X-100 once (PSD I), twice (PSD II), or with Triton X-100 and Sarkosyl (PSD III). (**H**–**J**) Wild-type (WT) DGKζ shows a greater spine localization compared with a mutant DGKζ that lacks the PSD-95-binding C terminus (ΔC). Cultured hippocampal neurons transfected with HA-DGKζ constructs and PSD-95-EGFP (days *in vitro*, DIV 17–18) were stained with HA and EGFP antibodies and used to measure the ratio of DGKζ signals at a spine versus an adjacent dendritic trunk. PSD-95-EGFP was co-transfected with DGKζ so that the amount of PSD-95 does not become a limiting factor. Data represent mean ± s.e.m. (WT, $n=18$ neurons; ΔC, $n=10$ neurons). $^{***}P<0.001$ (Student's *t*-test). Scale bar, 10 μm. (**K**–**M**) Knockdown of PSD-95 reduces spine localization of DGKζ. Cultured neurons were doubly transfected with HA-DGKζ and a PSD-95 knockdown construct (sh-PSD-95), or HA-DGKζ and empty sh-RNA vector and (sh-vec; DIV 14–20), and the spine/dendrite ratio of DGKζ signals were measured. Data represent mean ± s.e.m. (sh-vec, $n=13$ neurons; sh-PSD-95, $n=19$ neurons). $^{***}P<0.001$ (Student's *t*-test). Scale bar, 10 μm.

Before we explore the functions of the interaction between PSD-95 and DGKζ, we first determined the expression patterns of DGKζ proteins in rat brain, using a DGKζ-specific polyclonal antibody that we generated (Supplementary Figure S2). In immunoblot analysis, DGKζ protein expression was detected in various rat brain regions (Figure 1D). Consistently, DGKζ immunofluorescence was observed in various brain regions, including hippocampus and cerebellum (Supplementary Figure S3). Minimal signals were detected in brain slices from DGKζ-deficient mice (Supplementary Figure S3), indicating the specificity of the antibody. DGKζ expression gradually increased during postnatal rat brain development (Figure 1E). In subcellular fractions of the rat brain, DGKζ was detected in synaptic fractions, including crude synaptosomal, synaptic membrane, and synaptic vesicle fractions (Figure 1F). Notably, DGKζ was highly enriched in postsynaptic density (PSD; electron-dense postsynaptic multiprotein complexes) fractions, to an extent comparable to PSD-95 (Figure 1G), indicating that DGKζ is tightly associated with the PSD.

The subcellular fractionation patterns of PSD-95 and DGKζ (Figure 1F) indicate that PSD-95 is mainly localized at synaptic fractions, whereas DGKζ is not. We thus reasoned that DGKζ may depend on PSD-95 interaction for its synaptic localization. Indeed, wild-type (WT) DGKζ expressed in cultured hippocampal neurons showed a greater localization at dendritic spines, compared with a mutant that lacks PSD-95 binding (DGKζΔC) (Figure 1H–J), suggesting that PSD-95 promotes synaptic localization of DGKζ. Of note, some of DGKζΔC signals colocalized with PSD-95 in dendrites (Figure 1I). This is most likely to be caused by the association of DGKζΔC with endogenous DGKζ, which is capable of binding to PSD-95, rather than a C terminus-independent DGKζ binding to PSD-95 (Supplementary Figure S4A). In support of this possibility, DGKζ could form self-multimers, as shown by the co-immunoprecipitation of differentially tagged DGKζ proteins (Supplementary Figure S4B). In further support of the role for PSD-95 in synaptic DGKζ localization, knockdown of PSD-95 significantly decreased spine localization of DGKζ (Figure 1K–M; Supplementary Figure S5A). DGKζ has also been shown to interact with another PDZ protein, γ1-syntrophin (Hogan *et al*, 2001). However, the role for γ1-syntrophin in synaptic DGKζ localization is unclear because γ1-syntrophin is detected mainly in the endoplasmic reticulum of neuronal cell bodies (Alessi *et al*, 2006).

DGKζ is detected mainly in dendrites and postsynaptic sites

We next determined the subcellular and ultrastructural localization of DGKζ. In cultured hippocampal neurons, DGKζ was detected in MAP2 (a dendritic marker)-positive dendrites, although relative weak signals were also detected in MAP2-negative axons (Figure 2A). In dendrites, DGKζ showed a widespread subcellular distribution, with some of the DGKζ signals being colocalized with PSD-95 (an excitatory postsynaptic marker) and synapsin I (a presynaptic marker) (Figure 2B and C).

Ultrastructural localizations of DGKζ were determined by electron microscopic analysis. DGKζ was detected mainly in the cell body and proximal dendrites (Figure 2D) as well as distal dendrites (Figure 2E). In contrast, DGKζ was rarely detected in axonal compartments (Figure 2F). The majority of dendritic spines contained DGKζ signals in regions including the PSD, whereas axon terminals in contact with dendritic spines were usually devoid of detectable DGKζ signals

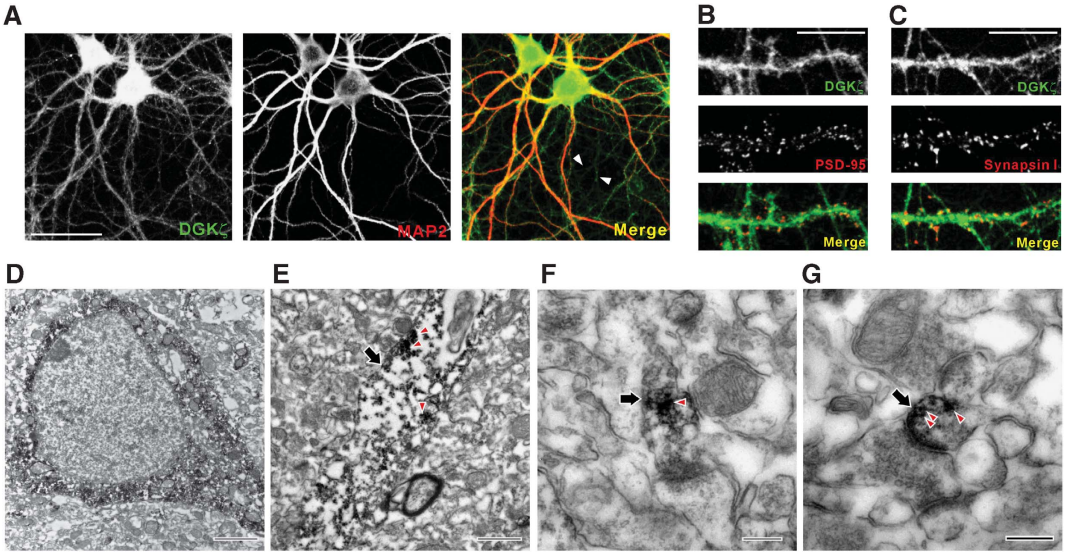

Figure 2 Subcellular and ultrastructural localization of DGKζ in neurons. (**A**) DGKζ localizes to MAP2 (a dendritic marker protein)-positive dendrites as well as MAP2-negative axons (arrowheads). Cultured hippocampal neurons (DIV 21) were stained with DGKζ (1521) and MAP2 antibodies. Scale bar, 50 μm. (**B**, **C**) DGKζ colocalizes with PSD-95 (an excitatory postsynaptic marker) and synapsin I (a presynaptic marker). Note that DGKζ shows widespread distribution patterns including the dendritic trunk and PSD-95/synapsin I-positive synaptic sites. Scale bar, 10 μm. (**D**–**G**) Ultrastructural localization of DGKζ in somatodendritic regions and dendritic spines of CA1 pyramidal neurons. Note that DGKζ signals, shown as dark DAB precipitates (arrowheads), are present mainly in the cell body and proximal dendrites (D) as well as distal dendrites (E; indicated by an arrow), whereas axons rarely contain DGKζ signals (F; an arrow indicates an axon terminal). In addition, DGKζ is detected in the majority of dendritic spines in regions including the PSD, whereas axon terminals in contact with dendritic spines rarely contain DGKζ signals (G; an arrow indicates a spine synapse). Scale bars; 2 μm (D), 1 μm (E), and 0.2 μm (F, G).

(Figure 2G). These results suggest that DGKζ is present mainly in postsynaptic compartments.

DGKζ-dependent spine regulation requires its catalytic activity and PSD-95 binding

Production of DAG at neuronal synapses can occur through the activation of PLC-coupled GPCRs, including mGluRs (Conn and Pin, 1997) and non-GPCRs such as NMDARs, a key mediator of excitatory synaptic transmission (Reyes-Harde and Stanton, 1998; Choi *et al*, 2005; Horne and Dell'Acqua, 2007). Synaptic proteins that exert an effect in the downstream of DAG such as α1-chimaerin and MARCKS have been implicated in the regulation of dendritic spines (Calabrese and Halpain, 2005; Buttery *et al*, 2006), which are actin-rich tiny protrusions on neuronal dendrites (Calabrese *et al*, 2006; Tada and Sheng, 2006; Bourne and Harris, 2008). In addition, PSD-95, which is in direct association with DGKζ, is a key regulator of spine morphogenesis (Tada and Sheng, 2006). We thus tested whether DGKζ is involved in the regulation of dendritic spines. DGKζ overexpression in cultured hippocampal neurons (days *in vitro* or DIV 15–22) significantly increased the density, but not length and width, of dendritic spines (Figure 3A–E). In contrast, DGKζ mutants (ΔC and kinase-dead) that lack PSD-95 binding and kinase activity, respectively, had no effect on spine density (Figure 3A–E). These results suggest that DGKζ increases spine density through mechanisms requiring its synaptic localization and catalytic activity.

Because DGKζ overexpression increases spine density, we reasoned that a reduced expression of DGKζ may negatively regulate spine density. Indeed, cultured neurons with DGKζ knocked down by RNAi (DIV 15–19) displayed a significantly reduced spine density, compared with controls (Figure 4A and B; Supplementary Figures S5B and S5C). Spine length and width, however, were unaffected (Figure 4C and D). The reduced spine density could be rescued by co-transfection of a WT DGKζ expression construct resistant to sh-DGKζ, but not by a kinase-dead construct (Figure 4A–D; Supplementary Figure S5D). DGKζ knockdown also reduced the number of PSD-95-positive dendritic spines (Figure 4E and F). However, DGKζ knockdown did not reduce spine localization of PSD-95 (Figure 4G), suggesting that DGKζ knockdown does not affect synaptic PSD-95 localization. These results suggest that DGKζ is important for the maintenance of dendritic spines in a manner requiring its catalytic activity.

Reduced PA production and spine density in DGKζ−/− mice

To determine whether the results obtained from cultured neurons have relevance *in vivo*, we analysed DGKζ−/− mice, which exhibit enhanced T-cell responses caused by reduced DAG conversion to PA (Zhong *et al*, 2003). We observed a similar reduction in PA production in DGKζ−/− hippocampal slices, when synaptic DAG production was stimulated with DHPG, a group I mGluR agonist (Figure 5A). In contrast, basal PA levels in DGKζ−/− slices were not significantly different from WT mice, although there was a tendency for a decrease (Figure 5A). In addition to measuring PA production, we compared expression levels of DGKζ proteins and other synaptic proteins in the whole brain of DGKζ−/− and WT mice. Although DGKζ expression could not be detected in DGKζ−/− brain, expression levels of other synaptic proteins were unchanged (Supplementary Figure S6).

For spine analysis, hippocampal CA1 pyramidal neurons were visualized by ballistic delivery of DiI-coated particles (Gan *et al*, 2000). Consistent with the results from cultured neurons, spine density, but not spine head area, was significantly reduced (∼30%) in DGKζ−/− pyramidal neurons, compared with WT controls (Figure 5B–D), suggesting that DGKζ is required for the maintenance of dendritic spines *in vivo*.

Reduced excitatory synaptic transmission in DGKζ−/− mice

We next tested whether the reduction of spine density in DGKζ−/− mice is accompanied by functional reduction in excitatory synaptic transmission. The frequency, but not

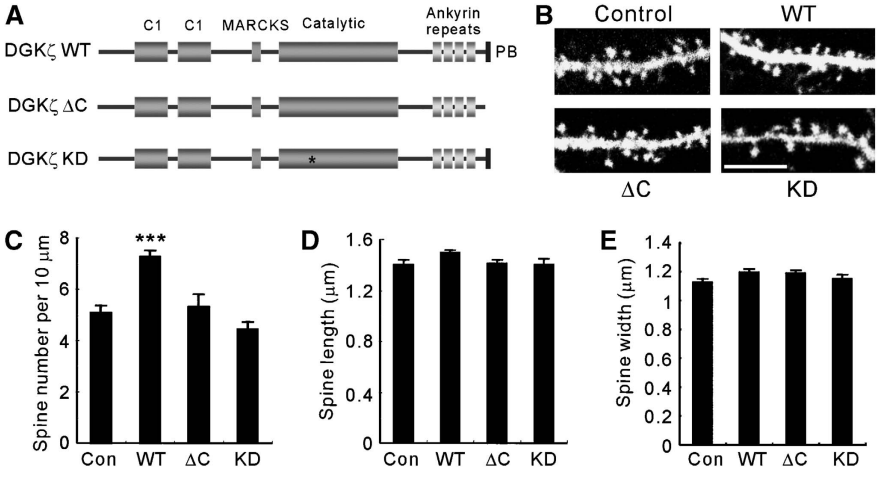

Figure 3 Overexpression of DGKζ increases spine density in cultured neurons. (**A**) Domain structure of DGKζ variants. KD, kinase-dead mutant. (**B**) Increased spine density by overexpression of WT DGKζ, but not by ΔC and KD mutants. Cultured hippocampal neurons transfected with HA-DGKζ (WT and mutants) and EGFP, or EGFP alone (control; DIV 15–22), were stained with EGFP antibodies. Scale bar, 10 μm. (**C–E**) Quantification of spine density, length, and width from the results in (B). Data represent mean ± s.e.m. (Control, 5.06 ± 0.28 spines per 10 μm dendrite. $n = 37$; WT, 7.27 ± 0.26, $n = 31$; ΔC, 5.33 ± 0.45, $n = 22$; KD, 4.46 ± 0.28, $n = 16$). ***$P < 0.001$ (Student's *t*-test).

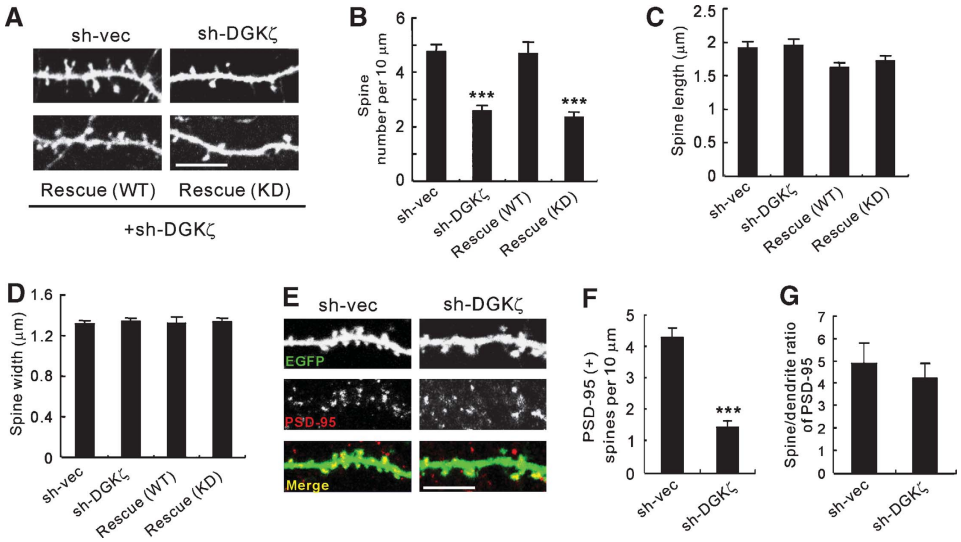

Figure 4 Knockdown of DGKζ decreases spine density. (**A**) Reduced spine density by DGKζ knockdown, and rescue of the effect requiring catalytic activity. Neurons were transfected with an shRNA DGKζ knockdown construct (sh-DGKζ), or vector alone (sh-vec; DIV 15–19), and stained with EGFP antibodies for spine visualization. Rescue expression constructs were doubly transfected with sh-DGKζ. Scale bar, 10 μm. (**B**–**D**) Quantification of the results in (A). Mean ± s.e.m. (sh-vec, 4.74 ± 0.26, $n = 19$; sh-DGKζ, 2.56 ± 0.21, $n = 18$; WT rescue, 4.67 ± 0.42, $n = 8$; KD rescue, 2.36 ± 0.19, $n = 26$). $^{***}P < 0.001$ (Student's *t*-test). (**E**) DGKζ knockdown reduces the number of PSD-95-positive dendritic spines. Neurons were transfected with sh-DGKζ or sh-vec (DIV 15–19), and stained for PSD-95 and EGFP. Scale bar, 10 μm. (**F**) Quantification of the number of PSD-95-positive dendritic spines from the results in (E). Mean ± s.e.m. (sh-vec, 4.27 ± 0.31, $n = 24$; sh-DGKζ, 1.42 ± 0.2, $n = 25$). $^{***}P < 0.001$ (Student's *t*-test). (**G**) Quantification of the spine/dendrite ratio of PSD-95 from the results in (E). Mean ± s.e.m. (sh-vec, 4.88 ± 0.89, $n = 16$; sh-DGKζ, 4.19 ± 0.68, $n = 16$).

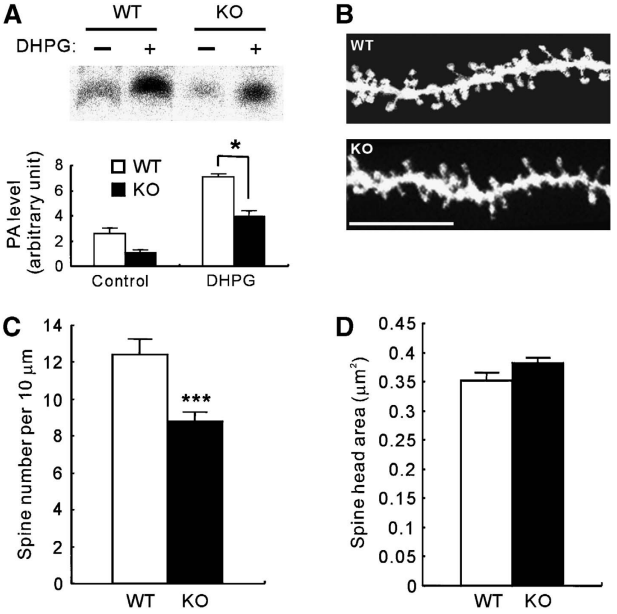

Figure 5 Reduced PA production and spine density in DGKζ−/− mice. (**A**) Reduced PA production in DGKζ−/− hippocampus. PA production was induced by the treatment of DHPG (a group I mGluR agonist) on WT and DGKζ−/− hippocampal slices. Data represent mean ± s.e.m. (basal-WT, 2.57 ± 0.48, $n = 3$; basal-KO, 1.05 ± 0.25, $n = 3$; DHPG-WT, 7.06 ± 0.28, $n = 3$; DHPG-KO, 3.96 ± 0.44, $n = 3$). $^{*}P < 0.05$ (Student's *t*-test). (**B**) Reduced spine density in DGKζ−/− CA1 pyramidal neurons. Spines in WT and DGKζ−/− pyramidal neurons were labelled by ballistic delivery of DiI-coated particles to hippocampal slices (3 weeks old). Scale bar, 10 μm. (**C**, **D**) Quantification of the results from (B) reveals a reduction in spine density, but not in spine head area, in DGKζ−/− neurons. Mean ± s.e.m. (WT, 12.41 ± 0.87 spines per 10 μm dendrite, $n = 27$ neurons from three mice; KO, 8.79 ± 0.51, $n = 30$, three mice). $^{***}P < 0.01$ (Student's *t*-test).

amplitude, of miniature excitatory postsynaptic currents (mEPSCs) was reduced (~44%) in DGKζ−/− CA1 pyramidal neurons (Figure 6A and B), suggesting that DGKζ is required for the maintenance of AMPA receptor-mediated spontaneous excitatory synaptic transmission. Miniature inhibitory postsynaptic currents (mIPSCs), however, were unaffected (Figure 6C and D). The slopes of AMPA receptor-mediated evoked fEPSPs plotted against the stimulation intensity were reduced at DGKζ−/− Schaffer collateral–CA1 pyramidal synapses (Figure 6E), consistent with the reduction in mEPSC frequencies. The paired-pulse facilitation (PPF) ratio was not changed at DGKζ−/− Schaffer collateral–CA1 pyramidal synapses (Figure 6F), suggesting that the reductions in AMPA receptor-mediated spontaneous and evoked responses were not caused by a reduction in presynaptic release probability. The ratio of AMPA receptor and NMDAR-mediated evoked EPSCs in DGKζ−/− CA1 pyramidal neurons was comparable to that of WT mice (Figure 6G and H), suggesting that DGKζ deficiency did not cause a change in the AMPA/NMDA ratio of excitatory transmission in synapses that escaped the reduction in number.

DGKζ regulates the maintenance but not formation of dendritic spines

The reduced spine density induced by DGKζ knockdown may be caused by either reduced spine formation and/or increased spine elimination. To address this issue, we monitored the dynamics of dendritic spines in live cultured neurons transfected with the DGKζ knockdown construct. DGKζ knockdown markedly increased the number of disappearing dendritic spines during the period of 2-h live imaging, compared with control neurons transfected with the empty knockdown vector (Figure 7A and B). Accordingly, the num-

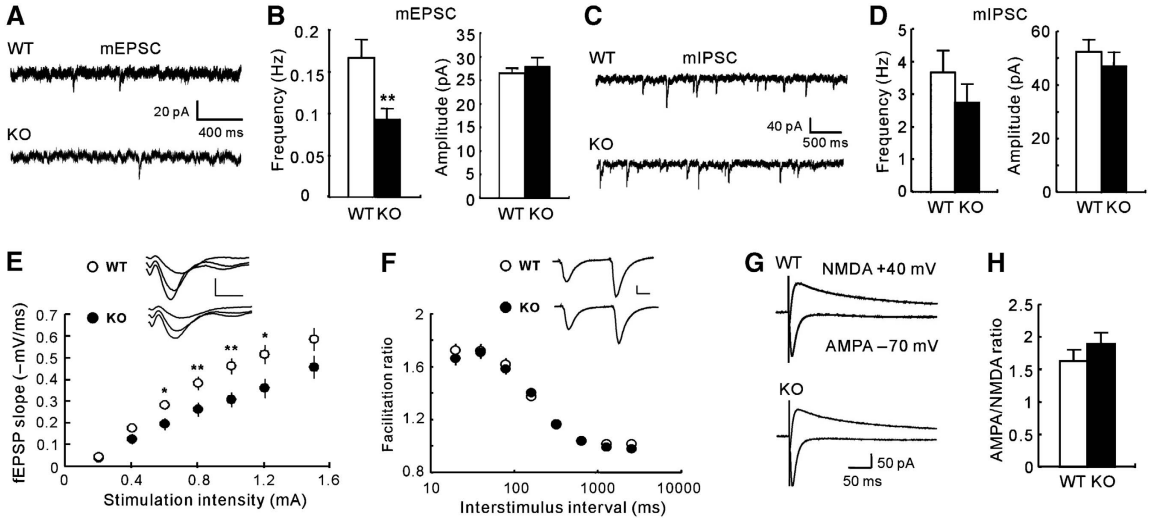

Figure 6 Reduced excitatory synaptic transmission in DGKζ−/− mice. (**A**, **B**) Reduced frequency, but not amplitude, of mEPSCs in DGKζ−/− CA1 pyramidal neurons. Mean ± s.e.m. (WT, 0.17 ± 0.02 Hz, $n = 27$ cells from seven mice; KO, 0.09 ± 0.01 Hz, $n = 26$, four mice). $^{**}P < 0.01$ (Student's *t*-test). (**C**, **D**) Normal frequency and amplitude of mIPSCs in DGKζ−/− CA1 neurons. (WT, $n = 10$ cells from three mice; KO, $n = 9$, three mice). (**E**) Reduced AMPA receptor-mediated evoked synaptic transmission at DGKζ−/− Schaffer collateral–CA1 pyramidal synapses. The synaptic input–output relationship was obtained by plotting fEPSP slopes against stimulation intensities. $n = 27$ slices from 10 KO mice and 31 slices from 11 WT mice. Scale bar, 4 ms/0.4 mV. (**F**) Normal paired-pulse facilitation ratio at DGKζ−/− Schaffer collateral–CA1 pyramidal synapses. Facilitation ratios were plotted against interstimulus intervals. $n = 38 \sim 39$ slices from 13 ∼ 14 mice. Scale bar, 10 ms/0.5 mV. (**G**, **H**) Normal ratio of AMPA and NMDA receptor-mediated EPSCs. Mean ± s.e.m. (WT, $n = 11$ cells from seven mice; KO, $n = 9$, seven mice). AMPA and NMDA receptor-mediated responses were recorded under voltage clamp with a holding potential of −70 and +40 mV, respectively.

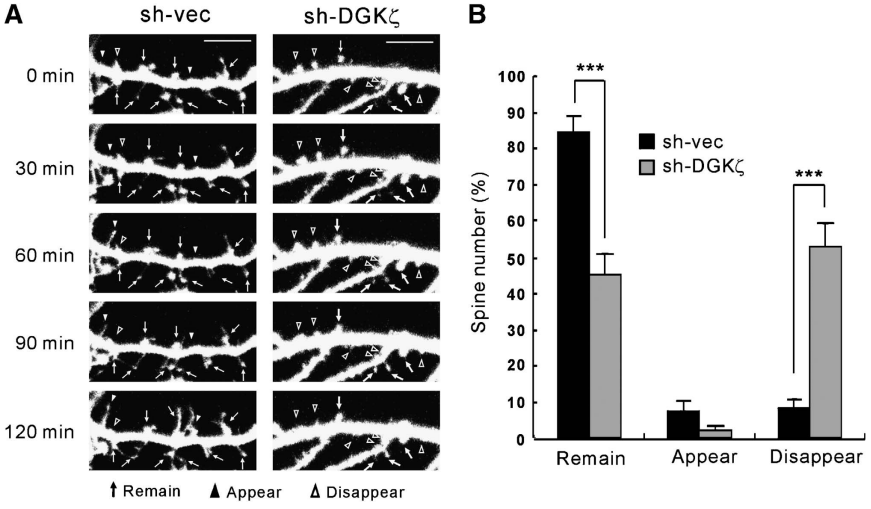

Figure 7 DGKζ regulates the maintenance but not formation of dendritic spines. (**A**) DGKζ knockdown markedly increases the number of disappearing spines. Cultured neurons were transfected with sh-DGKζ or control vector (sh-vec), at DIV 13, followed by time-lapse imaging of EGFP-positive live neurons at DIV 17 for 2 h. Open arrowheads, disappearing spines; filled arrowheads, appearing spines; arrows: spines remained after the 2-h imaging. Scale bar, 10 μm. (**B**) Quantification of the results in (A). Percentages of remaining, appearing, and disappearing protrusions are indicated (the sum of remained, appeared, and disappeared spines was used as the total number of spines). Mean ± s.e.m. sh-vec (remain, 84.6 ± 4.16; appear, 7.25 ± 2.86; disappear, 8.14 ± 2.38; $n = 264$ spines from five neurons); sh-DGKζ (remain, 45.14 ± 5.57; appear, 1.95 ± 1.22; disappear, 52.9 ± 6.35; $n = 204$ spines from six neurons). $^{***}P < 0.001$ (Student's *t*-test).

ber of remaining dendritic spines after 2-h imaging was significantly decreased in DGKζ knockdown neurons (Figure 7A and B). In contrast, the number of appearing spines was not significantly decreased in DGKζ knockdown neurons, although there was a tendency for a decrease (Figure 7A and B). Because the overall number of disappearing spines is much greater than that of appearing spines in DGKζ knockdown neurons, DGKζ knockdown seems to reduce spine density mainly through spine elimination.

PKC inhibition does not block DGKζ knockdown-induced spine density reduction

Decreased expression of DGKζ in cultured neurons may lead to both an increase in DAG levels and a decrease in PA levels.

A well-known downstream effector of DAG is PKC. In addition, MARCKS, a substrate of PKC, is required for the spine shrinkage induced by phorbol ester (a PKC activator) in cultured neurons (Calabrese *et al*, 2006). These results suggest that DGKζ knockdown may reduce spine density through the PKC signalling pathway. To this end, we tested whether PKC inhibition reduces the spine reduction induced by DGKζ knockdown. However, incubation of cultured neurons with Gö6976, a specific inhibitor of PKC, during the period of DGKζ knockdown (DIV 15–19) did not significantly reduce the effect of DGKζ knockdown (Figure 8A and B). The effectiveness of Gö6976 as a PKC inhibitor was verified in heterologous cells and neurons stimulated with PMA (a PKC activator) (Supplementary Figure S7). These results indicate that PKC is minimally involved in DGKζ knockdown-induced reduction in spine density.

Discussion

Our results suggest that PSD-95 recruits DGKζ to excitatory synapses to tightly control synaptic DAG conversion to PA. Given the direct interaction of PSD-95 with NMDARs, a strong stimulator of PLC activation and DAG production (Horne and Dell'Acqua, 2007), PSD-95 may target DGKζ close to NMDARs to tightly couple DAG production to its conversion to PA. Consistently, a recent study has demonstrated that DGKs are targeted to GPCRs by their interactions with β-arrestin, a signalling adaptor/scaffolding protein (Nelson *et al*, 2007).

PSD-95 is known to be linked to other proteins in the DAG signalling pathway in the brain. Shank, a synaptic scaffold linked to PSD-95 through GKAP, interacts directly with PLCβ and indirectly with mGluRs (a stimulator of PLCβ) (Tu *et al*, 1999; Hwang *et al*, 2005). These interactions along with our results suggest that PSD-95 may function as a scaffold to organize the synaptic DAG signalling pathway into a macromolecular complex, which contains proteins involved in PLC stimulation (NMDARs and mGluRs), DAG generation (PLCβ), and DAG-to-PA conversion (DGKζ). This is reminiscent of the INAD (a multi-PDZ protein)-dependent protein complex in the *Drosophila* phototransduction pathway that contains PLC, TRP channels (a DAG effector), and ePKC (a negative regulator of TRP channel), and which is thought to promote the high sensitivity, fast activation/deactivation, and feedback modulation of the signalling pathway (Montell, 1999).

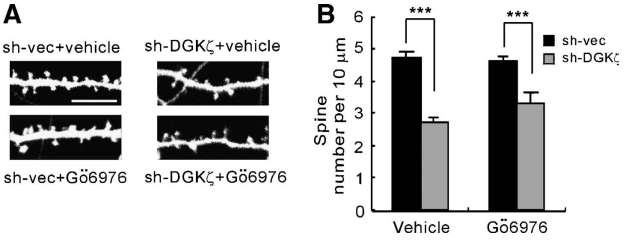

Figure 8 PKC inhibition does not block DGKζ knockdown-induced spine density reduction. (**A**) PKC inhibition does not affect DGKζ knockdown-induced spine reduction. Cultured neurons transfected with sh-DGKζ or sh-vec (DIV 15–19), were treated with Gö6976 (200 nM) or vehicle (DMSO; DIV 15–19). (**B**) Quantification of the results in (B). Mean ± s.e.m. (sh-vec/vehicle, 4.72 ± 0.18, $n = 39$; sh-DGKζ/vehicle, 2.71 ± 0.17, $n = 34$; sh-vec/Gö6976, 4.62 ± 0.16, $n = 60$; sh-DGKζ/Gö6976, 3.32 ± 0.33, $n = 33$).

Such examples, however, have not been identified in higher organisms.

Our data indicate that DGKζ forms a complex with all four known members of the PSD-95 family in brain (Figure 1), consistent with the *in vitro* results (Supplementary Figure S1). PSD-95 family proteins have been suggested to have overlapping as well as distinct functions with regard to their spatiotemporal expression patterns, protein interactions, and regulation of synaptic transmission (Sans *et al*, 2000, 2001; Valtschanoff *et al*, 2000; Rumbaugh *et al*, 2003; Townsend *et al*, 2003; Kim and Sheng, 2004; Elias *et al*, 2006; Fitzjohn *et al*, 2006; Schluter *et al*, 2006; Elias and Nicoll, 2007). For instance, targeted truncation of PSD-95 in mice does not affect AMPA receptor-mediated synaptic transmission (Migaud *et al*, 1998), most likely due to the compensation by other PSD-95 family members. Therefore, the promiscuous interaction of DGKζ with PSD-95 family proteins may contribute to the stable maintenance of dendritic spines and excitatory transmission.

Our results indicate that DGKζ is detected mainly in dendrites and postsynaptic sites, consistent with the DGKζ-dependent spine regulation. However, a small portion of DGKζ proteins is also detected in axon terminals, consistent with the localization of DGKζ in the LP2 (synaptic vesicle-enriched) fraction. Therefore, we cannot exclude the possibility that the reductions in spine density and synaptic transmission at DGKζ−/− synapses are caused, at least in part, by presynaptic defects, although the presynaptic release probability, as measured by PPF, appears normal in the knockout animals.

Our data from cultured neurons and DGKζ−/− mice suggest that DGKζ-mediated synaptic conversion of DAG to PA is required for the maintenance of dendritic spines. The reduced spine density may result from enhanced actions of DAG on synaptic effectors such as PKC. However, inhibition of PKC during DGKζ knockdown did not significantly reduce the effect of DGKζ knockdown. This suggests that PKC may not be the major pathway mediating the spine-reducing effect of DGKζ knockdown. However, it is possible that, even in the absence of the influences of PKC pathway, other DAG pathways may still be sufficient to induce spine reduction under the condition of elevated DAG levels. A possible non-PKC DAG effector is α1-chimaerin, a Rac1 GTPase-activating protein known to mediate DAG-dependent spine pruning (Buttery *et al*, 2006). Alternatively, because DGKζ deficiency leads to a decrease in PA production (Figure 5), insufficient activation of downstream PA effectors may inhibit spine maintenance. Previous studies have identified a large number of PA effectors, including Rac1, PAK1, PIP5K (phosphatidylinositol-4-phosphate 5-kinase), RasGAP, sphingosine kinase, atypical PKC, Raf-1, PKCε, PP1c (the catalytic subunit of protein phosphatase-1), mTOR, Opi1p, $p47^{phox}$, n-chimaerin, and β2-chimaerin. Of these proteins, Rac1 and PAK1 have been strongly implicated in the regulation of dendritic spines and F-actin, the main cytoskeleton of dendritic spines (Calabrese *et al*, 2006; Tada and Sheng, 2006; Bourne and Harris, 2008). Therefore, our study suggests the PA effectors listed above as potential regulators of dendritic spines.

In conclusion, our results suggest that synaptic DAG-to-PA conversion promoted by PSD-95-dependent synaptic targeting of DGKζ tightly regulates local DAG levels for the maintenance of normal spine density and excitatory

synaptic transmission. Our study suggests a novel mechanism by which local DAG concentration can be efficiently regulated by scaffolding protein-dependent localization of DAG-converting enzymes to the vicinity of DAG-generating proteins, which may be employed by various other subcellular sites.

Materials and methods

Constructs

The PDZ2 domain of PSD-95 (aa 89–299) in pBHA was used to screen a human brain cDNA library in pACT2 (Clontech). DGKζ (aa 923–929), wild type, and mutant (V929A) were annealed into pBHA. Rat DGKζ expression constructs (HA-DGKζ WT and ΔC; WT, full length; ΔC, deletion of the last four residues) were subcloned into pcDNA3.1-HA. EGFP-DGKζ was generated by subcloning full-length DGKζ into pEGFP-C1, kinase-dead (G354D) DGKζ was generated using QuickChange kit (Stratagene). The DGKζ knockdown construct was generated by subcloning nt 159–177 (CAGGAAAGCCATCACCAAG) into pSUPER.gfp/neo (OligoEngine). The PSD-95 knockdown construct was generated by subcloning nt 415–433 (GAGGCAGGTTCCATCGTTC) into pSUPER.gfp/neo (OligoEngine). GW1-PSD-95, GW1-Myc-PSD-95, and GW1-PSD-95-EGFP have been described (Kim *et al*, 1995; Hsueh *et al*, 1997; Arnold and Clapham, 1999).

Antibodies

GST-DGKζ (aa 661–929) was used to generate rabbit (1519) and guinea-pig (1521) polyclonal antibodies. The following antibodies have been reported: PSD-95 (SM55), PSD-95 (1402), EGFP (1167), PSD-93/chapsyn-110 (B9594), SAP97 (B9591), SAP102 (1445), and GRIP2 (1757). The other antibodies were purchased: Myc, HA, and synaptophysin (Santa Cruz), synapsin I (Chemicon), phospho-(Ser) PKC substrate (Cell Signaling Technology), and α-tubulin and MAP2 (Sigma, St Louis, MO).

Fractionation of rat brain lysates

Subcellular fractions of rat brains (6 weeks) were prepared as described (Huttner *et al*, 1983). PSD fractions were prepared as described (Cho *et al*, 1992).

Electron microscopy

Two male Sprague–Dawley rats (280–300 g) were deeply anaesthetized with sodium pentobarbital (80 mg/kg, i.p.) and intracardially perfused with a mixture of 4% paraformaldehyde and 0.01% glutaraldehyde in phosphate buffer (PB, pH 7.4). Hippocampus was removed and cut at 60 μm on a vibratome and then cryoprotected in 30% sucrose in PB overnight. Cryoprotected sections were frozen and thawed, and then treated with 3% H_2O_2 and 10% normal donkey serum. The sections were incubated overnight in the guinea-pig DGKζ antibodies (1521; 4 μg/ml) at room temperature and then with a biotinylated donkey anti-guinea-pig antibody (1:200; Jackson Immunoresearch) for 2 h. After washing, the sections were incubated with ExtrAvidin peroxidase (1:5000; Sigma), and the immunoperoxidase was visualized by nickel-intensified 3,3′-diaminobenzidine tetrahydrochloride. Sections were osmicated, dehydrated in graded alcohols, embedded with Durcupan ACM (Fluka, Buchs, Switzerland), and cured for 48 h at 60°C. Area containing pyramidal cell layer and stratum radiatum of the CA1 region was trimmed. Thin sections were cut, mounted on nickel grids, and stained with uranyl acetate and lead citrate. Grids were examined on a Hitachi H 7500 electron microscope at 80 kV accelerating voltage.

Neuron culture and transfection

Cultured neurons prepared from rat hippocampi at E18 were maintained in neurobasal medium supplemented with B27 (Life Technologies). Neurons were transfected using the calcium phosphate method.

PA analysis

Hippocampal slices were incubated in phosphate-free artificial cerebrospinal fluid for 1 h, followed by metabolic labelling with 10 μCi/ml of ^{32}P-orthophosphate (GE Healthcare Life Sciences) for 30 min in the presence of 1% ethanol at 30°C. Labelled slices were incubated with 100 μM DHPG for 20 min. Lipid extraction and thin layer chromatography were carried out as described previously (Nelson *et al*, 2007).

DiOlistic spine labelling and image analysis

Transcardially perfused 3-week-old mice brain slices were labelled by the ballistic delivery of the lipophilic dye DiI as described (Gan *et al*, 2000). After dye delivery, brain slices were kept in phosphate-buffered saline for 4 h to allow dye diffusion. *Z*-stacked images from the proximal stratum radiatum region of hippocampus were used for blind image analysis. Spines were defined by protrusions with a bulbous head wider than the neck and with length longer than 0.5 μm. Spine density was measured from 40- to 80-μm segments of secondary dendrites on ~1–2 dendrites per neuron. The narrowest point in the spine neck was defined as the border between spine head and neck. MetaMorph software (Molecular Devices) was used for quantitative analysis.

Electrophysiology

For whole-cell recordings, CA1 pyramidal cell was held at −70 mV using a MultiClamp 700B amplifier (Axon Instruments). Pipette solutions contained (in mM) 110 Cs-gluconate, 30 CsCl, 20 HEPES, 4 MgATP, 0.3 NaGTP, 4 NaVitC, 0.5 EGTA (10 EGTA for AMPA versus NMDAR ratio) for mEPSC, or 145 CsCl, 20 HEPES, 4 MgATP, 0.3 NaGTP, 10 EGTA for mIPSC. TTX (0.5 μM) and bicuculline (20 μM) were added to ACSF for mEPSC measurements, and bicuculline was replaced with CNQX (10 μM) and AP5 (50 μM) for mIPSC measurements. To obtain AMPA receptor-mediated EPSCs, neuron in ACSF with 100 μM picrotoxin was held at −70 mV and stimulated at 0.066 Hz. NMDAR-mediated EPSC was isolated by changing holding potential to +40 mV and adding 10 μM CNQX to ACSF. EPSC samples (~25–30) were averaged to obtain the AMPA/NMDA EPSC ratio.

Time-lapse imaging

Cultured neurons expressing sh-DGKζ, or control vector (sh-vec), were mounted in a chamber (Zeiss) where temperature (37°C) and CO_2 concentration (10%) were maintained during the recording. Images were acquired with an LSM510 confocal microscope (Zeiss) using a C-Apochromat ×63, 1.20 NA water-immersion objective. The laser power was attenuated to less than 3% to avoid fluorescence bleaching and neuronal toxicity, and images were taken every 10 min for 2 h.

Supplementary data

Supplementary data are available at *The EMBO Journal* Online (http://www.embojournal.org).

Acknowledgements

This study was supported by the National Creative Research Initiative Program of the Korean Ministry of Science and Technology (to EK), the Korea Research Foundation Grant (KRF-2006-312-C00360; to S-YC), the MRC Program of the Korea Science and Engineering Foundation (KOSEF: R13-2008-009-01001-0; to YCB), the United States National Institutes of Health (R01-CA95463; to MKT), and Huntsman Cancer Foundation (to MKT). We thank Dr Christopher Nelson for the help with the PA assay.

References

Alessi A, Bragg AD, Percival JM, Yoo J, Albrecht DE, Froehner SC, Adams ME (2006) Gamma-syntrophin scaffolding is spatially and functionally distinct from that of the alpha/beta syntrophins. *Exp Cell Res* **312:** 3084–3095

Alvarez VA, Sabatini BL (2007) Anatomical and physiological plasticity of dendritic spines. *Annu Rev Neurosci* **30:** 79–97

Arnold DB, Clapham DE (1999) Molecular determinants for subcellular localization of PSD-95 with an interacting K^+ channel. *Neuron* **23:** 149–157

Bourne JN, Harris KM (2008) Balancing structure and function at hippocampal dendritic spines. *Annu Rev Neurosci* **31:** 47–67

Brenman JE, Chao DS, Gee SH, McGee AW, Craven SE, Santillano DR, Wu Z, Huang F, Xia H, Peters MF, Froehner SC, Bredt DS (1996) Interaction of nitric oxide synthase with the postsynaptic density protein PSD-95 and alpha1-syntrophin mediated by PDZ domains. *Cell* **84:** 757–767

Buttery P, Beg AA, Chih B, Broder A, Mason CA, Scheiffele P (2006) The diacylglycerol-binding protein alpha1-chimaerin regulates dendritic morphology. *Proc Natl Acad Sci USA* **103:** 1924–1929

Calabrese B, Halpain S (2005) Essential role for the PKC target MARCKS in maintaining dendritic spine morphology. *Neuron* **48:** 77–90

Calabrese B, Wilson MS, Halpain S (2006) Development and regulation of dendritic spine synapses. *Physiology (Bethesda)* **21:** 38–47

Carlisle HJ, Kennedy MB (2005) Spine architecture and synaptic plasticity. *Trends Neurosci* **28:** 182–187

Cho KO, Hunt CA, Kennedy MB (1992) The rat brain postsynaptic density fraction contains a homolog of the *Drosophila* discs-large tumor suppressor protein. *Neuron* **9:** 929–942

Choi SY, Chang J, Jiang B, Seol GH, Min SS, Han JS, Shin HS, Gallagher M, Kirkwood A (2005) Multiple receptors coupled to phospholipase C gate long-term depression in visual cortex. *J Neurosci* **25:** 11433–11443

Cingolani LA, Goda Y (2008) Actin in action: the interplay between the actin cytoskeleton and synaptic efficacy. *Nat Rev Neurosci* **9:** 344–356

Conn PJ, Pin JP (1997) Pharmacology and functions of metabotropic glutamate receptors. *Annu Rev Pharmacol Toxicol* **37:** 205–237

Elias GM, Funke L, Stein V, Grant SG, Bredt DS, Nicoll RA (2006) Synapse-specific and developmentally regulated targeting of AMPA receptors by a family of MAGUK scaffolding proteins. *Neuron* **52:** 307–320

Elias GM, Nicoll RA (2007) Synaptic trafficking of glutamate receptors by MAGUK scaffolding proteins. *Trends Cell Biol* **17:** 343–352

Ethell IM, Pasquale EB (2005) Molecular mechanisms of dendritic spine development and remodeling. *Prog Neurobiol* **75:** 161–205

Fitzjohn SM, Doherty AJ, Collingridge GL (2006) Promiscuous interactions between AMPA-Rs and MAGUKs. *Neuron* **52:** 222–224

Funke L, Dakoji S, Bredt DS (2004) Membrane-associated guanylate kinases regulate adhesion and plasticity at cell junctions. *Annu Rev Biochem* **74:** 219–245

Gan WB, Grutzendler J, Wong WT, Wong RO, Lichtman JW (2000) Multicolor 'DiOlistic' labeling of the nervous system using lipophilic dye combinations. *Neuron* **27:** 219–225

Goto K, Kondo H (1996) A 104-kDa diacylglycerol kinase containing ankyrin-like repeats localizes in the cell nucleus. *Proc Natl Acad Sci USA* **93:** 11196–11201

Govek EE, Newey SE, Van Aelst L (2005) The role of the Rho GTPases in neuronal development. *Genes Dev* **19:** 1–49

Hayashi Y, Majewska AK (2005) Dendritic spine geometry: functional implication and regulation. *Neuron* **46:** 529–532

Hogan A, Shepherd L, Chabot J, Quenneville S, Prescott SM, Topham MK, Gee SH (2001) Interaction of gamma 1-syntrophin with diacylglycerol kinase-zeta. Regulation of nuclear localization by PDZ interactions. *J Biol Chem* **276:** 26526–26533

Horne EA, Dell'Acqua ML (2007) Phospholipase C is required for changes in postsynaptic structure and function associated with NMDA receptor-dependent long-term depression. *J Neurosci* **27:** 3523–3534

Hsueh YP, Kim E, Sheng M (1997) Disulfide-linked head-to-head multimerization in the mechanism of ion channel clustering by PSD-95. *Neuron* **18:** 803–814

Huttner WB, Schiebler W, Greengard P, De Camilli P (1983) Synapsin I (protein I), a nerve terminal-specific phosphoprotein. III. Its association with synaptic vesicles studied in a highly purified synaptic vesicle preparation. *J Cell Biol* **96:** 1374–1388

Hwang JI, Kim HS, Lee JR, Kim E, Ryu SH, Suh PG (2005) The interaction of phospholipase C-beta3 with Shank2 regulates mGluR-mediated calcium signal. *J Biol Chem* **280:** 12467–12473

Kennedy MB (2000) Signal-processing machines at the postsynaptic density. *Science* **290:** 750–754

Kim E, Niethammer M, Rothschild A, Jan YN, Sheng M (1995) Clustering of Shaker-type K^+ channels by interaction with a family of membrane-associated guanylate kinases. *Nature* **378:** 85–88

Kim E, Sheng M (2004) PDZ domain proteins of synapses. *Nat Rev Neurosci* **5:** 771–781

Matus A (2005) Growth of dendritic spines: a continuing story. *Curr Opin Neurobiol* **15:** 67–72

Migaud M, Charlesworth P, Dempster M, Webster LC, Watabe AM, Makhinson M, He Y, Ramsay MF, Morris RG, Morrison JH, O'Dell TJ, Grant SG (1998) Enhanced long-term potentiation and impaired learning in mice with mutant postsynaptic density-95 protein. *Nature* **396:** 433–439

Montell C (1999) Visual transduction in *Drosophila*. *Annu Rev Cell Dev Biol* **15:** 231–268

Nelson CD, Perry SJ, Regier DS, Prescott SM, Topham MK, Lefkowitz RJ (2007) Targeting of diacylglycerol degradation to M1 muscarinic receptors by beta-arrestins. *Science* **315:** 663–666

Nimchinsky EA, Sabatini BL, Svoboda K (2002) Structure and function of dendritic spines. *Annu Rev Physiol* **64:** 313–353

Reyes-Harde M, Stanton PK (1998) Postsynaptic phospholipase C activity is required for the induction of homosynaptic long-term depression in rat hippocampus. *Neurosci Lett* **252:** 155–158

Rhee SG (2001) Regulation of phosphoinositide-specific phospholipase C. *Annu Rev Biochem* **70:** 281–312

Rumbaugh G, Sia GM, Garner CC, Huganir RL (2003) Synapse-associated protein-97 isoform-specific regulation of surface AMPA receptors and synaptic function in cultured neurons. *J Neurosci* **23:** 4567–4576

Sabatini BL, Maravall M, Svoboda K (2001) Ca(2+) signaling in dendritic spines. *Curr Opin Neurobiol* **11:** 349–356

Sakane F, Imai S, Kai M, Yasuda S, Kanoh H (2007) Diacylglycerol kinases: why so many of them? *Biochim Biophys Acta* **1771:** 793–806

Sans N, Petralia RS, Wang YX, Blahos II J, Hell JW, Wenthold RJ (2000) A developmental change in NMDA receptor-associated proteins at hippocampal synapses. *J Neurosci* **20:** 1260–1271

Sans N, Racca C, Petralia RS, Wang YX, McCallum J, Wenthold RJ (2001) Synapse-associated protein 97 selectively associates with a subset of AMPA receptors early in their biosynthetic pathway. *J Neurosci* **21:** 7506–7516

Sattler R, Xiong Z, Lu WY, Hafner M, MacDonald JF, Tymianski M (1999) Specific coupling of NMDA receptor activation to nitric oxide neurotoxicity by PSD-95 protein. *Science* **284:** 1845–1848

Scannevin RH, Huganir RL (2000) Postsynaptic organization and regulation of excitatory synapses. *Nat Rev Neurosci* **1:** 133–141

Schluter OM, Xu W, Malenka RC (2006) Alternative N-terminal domains of PSD-95 and SAP97 govern activity-dependent regulation of synaptic AMPA receptor function. *Neuron* **51:** 99–111

Schubert V, Dotti CG (2007) Transmitting on actin: synaptic control of dendritic architecture. *J Cell Sci* **120:** 205–212

Sekino Y, Kojima N, Shirao T (2007) Role of actin cytoskeleton in dendritic spine morphogenesis. *Neurochem Int* **51:** 92–104

Sheng M, Hoogenraad CC (2007) The postsynaptic architecture of excitatory synapses: a more quantitative view. *Annu Rev Biochem* **76:** 823–847

Sternweis PC, Smrcka AV, Gutowski S (1992) Hormone signalling via G-protein: regulation of phosphatidylinositol 4,5-bisphosphate hydrolysis by Gq. *Philos Trans R Soc Lond B Biol Sci* **336:** 35–41; discussion 41–42

Tada T, Sheng M (2006) Molecular mechanisms of dendritic spine morphogenesis. *Curr Opin Neurobiol* **16:** 95–101

Topham MK (2006) Signaling roles of diacylglycerol kinases. *J Cell Biochem* **97:** 474–484

Townsend M, Yoshii A, Mishina M, Constantine-Paton M (2003) Developmental loss of miniature *N*-methyl-D-aspartate receptor currents in NR2A knockout mice. *Proc Natl Acad Sci USA* **100:** 1340–1345

Tsay D, Yuste R (2004) On the electrical function of dendritic spines. *Trends Neurosci* **27:** 77–83

Tu JC, Xiao B, Naisbitt S, Yuan JP, Petralia RS, Brakeman P, Doan A, Aakalu VK, Lanahan AA, Sheng M, Worley PF (1999) Coupling of mGluR/Homer and PSD-95 complexes by the Shank family of postsynaptic density proteins. *Neuron* **23:** 583–592

Valtschanoff JG, Burette A, Davare MA, Leonard AS, Hell JW, Weinberg RJ (2000) SAP97 concentrates at the postsynaptic density in cerebral cortex. *Eur J Neurosci* **12:** 3605–3614

Zhong XP, Hainey EA, Olenchock BA, Jordan MS, Maltzman JS, Nichols KE, Shen H, Koretzky GA (2003) Enhanced T cell responses due to diacylglycerol kinase zeta deficiency. *Nat Immunol* **4:** 882–890